

# Dynamical friction on satellite galaxies

Michiko FUJII

*Department of Astronomy, Graduate School of Science, the University of Tokyo, Tokyo, 113*

*fujii@astron.s.u-tokyo.ac.jp*

Yoko FUNATO

*General Systems Studies, Graduate Division of International and Interdisciplinary Studies,*

*University of Tokyo, Tokyo, 153*

*funato@chianti.c.u-tokyo.ac.jp*

and

Junichiro MAKINO

*Department of Astronomy, Graduate School of Science, the University of Tokyo, Tokyo, 113*

*makino@astron.s.u-tokyo.ac.jp*

(Received ; accepted )

## Abstract

For a rigid model satellite, Chandrasekhar's dynamical friction formula describes the orbital evolution quite accurately, when the Coulomb logarithm is chosen appropriately. However, it is not known if the evolution of a real satellite with the internal degree of freedom can be described by the dynamical friction. We performed  $N$ -body simulation of the orbital evolution of a self-consistent satellite galaxy within a self-consistent parent galaxy. We found that the orbital decay of the simulated satellite is significantly faster than the estimate from the dynamical friction formula. The main cause of this discrepancy is that the stars stripped out of the satellite are still close to the satellite, and increase the drag force on the satellite through two mechanisms. One is the direct drag force from particles in the trailing tidal arm. The other is the indirect effect that the particles which remain close to the satellite enhances the dynamical friction. Dynamical friction operates on the total mass of the stars which move together, no matter whether they are gravitationally bound or not.

**Key words:** galaxies: evolution — galaxies: interactions — galaxies: kinematics and dynamics — methods: numerical — stellar dynamics

## 1. INTRODUCTION

The evolution of satellite galaxies has been studied by a number of researchers both theoretically and using numerical simulations. However, even though it is basic and a simple

problem, our understanding is still rather limited.

Using  $N$ -body simulation of a rigid satellite within an  $N$ -body model of the parent galaxy, van den Bosch et al. (1999) found that the orbital eccentricity of a satellite galaxy tends to be roughly constant. Previous theoretical studies based on Chandrasekhar's dynamical friction formula (Chandrasekhar 1943) predicted circularization of the orbit. Thus, there was rather serious qualitative difference between the simulation result and the theoretical model.

Hashimoto, Funato, & Makino (2003, hereafter H03) showed that Chandrasekhar's dynamical formula does give the result which is consistent with the simulation result, when the integration over an impact parameter is carried out correctly. The dynamical friction formula is given by

$$\mathbf{F}_d \sim -\frac{16\pi^2}{3}G^2\rho M^2 \log \Lambda \mathbf{v}_M. \quad (1)$$

Where the Coulomb logarithm  $\log \Lambda$  is given by

$$\log \Lambda = \log \left( \frac{b_{\max}}{b_{\min}} \right). \quad (2)$$

Here,  $b_{\max}$  and  $b_{\min}$  are the maximum and the minimum impact parameters for gravitational encounters between the satellite galaxy and the field stars in the parent galaxy. For the lower cutoff, it is natural to set  $b_{\min}$  to the order of the virial radius of the satellite galaxy (White 1976). For the upper cutoff, in many studies the size of the parent galaxy has been used (e.g., Murai & Fujimoto 1980; Helmi et al. 1999; Johnston et al. 1995).

H03 pointed out that, if the integration over all encounters is correctly performed, the discrepancy between  $N$ -body simulation result and the model with analytic estimate disappears. The exact integration over all encounters generally resulted in the dynamical friction term smaller than the value given by equation (1) and (2), simply because the density drops off at large radii. The use of equation (2) with the cutoff distance at the size of the parent galaxy is equivalent to assume that the parent galaxy is a sphere of the same size and with a constant density same as the local density around the satellite. Also, it implies that the orbit of the satellite is a straight line. However, since the density drops off and the orbit of the satellite is not a straight line, the actual dynamical friction is smaller. If we set the cutoff radius as the distance of the satellite from the center of the parent galaxy, equation (1) gives the result in good agreement with the  $N$ -body simulation.

H03 resolved the discrepancy between the theoretical and numerical results for the case of a rigid satellite. One of the reasons to construct a theoretical model for the orbital evolution due to dynamical friction is to study the evolution of the internal structure of the satellite galaxies. When we want to study the evolution of a satellite galaxy like LMC/SMC or Sagittarius dwarf, we want to use the number of particles as large as possible to model the dwarf. To achieve this goal, we model the parent galaxy by a fixed potential, and use the dynamical friction formula to model the orbital evolution. This technique has been used by a number of researchers (Bullock

& Johnston 2005; Johnston et al. 1995; Ibata & Lewis 1998; Portegies Zwart et al. 2004).

However, there is no guarantee that the orbital evolution of a live satellite is correctly described by the dynamical friction formula. Jiang and Binney (2000) compared the result of a fully self-consistent  $N$ -body simulation and a simplified model equation in which dynamical friction and tidal mass loss are taken into account. The agreement was not ideal. However, here, at least part of the cause of the discrepancy is the use of a constant Coulomb logarithm in their model equation, which resulted in the overestimation of the effect of dynamical friction.

In this paper we compare the result of self-consistent  $N$ -body simulation of orbital decay of a satellite with the dynamical friction formula proposed by H03. This paper is organized as follows. In section 2 we describe the simulation method and initial conditions. In section 3 we give the result. The agreement between the orbit obtained using model equation and simulation result is rather poor, and the model equation gave the orbital decay significantly slower than that observed in the  $N$ -body simulation. In section 4 we investigate the possible causes for this discrepancy. The difference between the self-consistent calculation and  $N$ -body simulations in which the satellites are treated as rigid bodies is the presence of the particles which originally were part of the satellite and then stripped out. These stripped particles might exert the drag force to the main body of the satellite, either through direct gravitational force or indirectly through modifying the distribution of field particles. We measured these direct and indirect effects, and found that both contributions are significant. The combined effect explains the discrepancy between the model calculation and  $N$ -body simulation. Section 5 is for discussions. We discuss the implication of our result on the studies of subhalos, dwarf galaxies and star clusters.

## 2. Numerical methods

### 2.1. Initial condition

We consider a simple problem of one spherical satellite galaxy orbiting in a spherical parent galaxy.

We adopted a King model with non-dimensional central potential  $W_0 = 9$  as the model of the parent galactic halo and  $W_0 = 7$  as that of the satellite halo. The system of units is the Heggie unit (Heggie & Mathieu 1986), where the gravitational constant  $G$  is 1 and the mass and the binding energy of the parent are 1 and 0.25, respectively. Initially, the satellite is placed at distance 1.5 from the center of the parent galaxy, with the velocity of 0.45. Assuming that the parent galaxy represents our Galaxy with total mass  $M = 10^{12} M_\odot$  and the circular velocity  $V_c = 250 \text{ km s}^{-1}$ , the initial distance and velocity of the satellite galaxy are 60 kpc and 140 km  $\text{s}^{-1}$ . Unit time in the Heggie unit corresponds to 130 Myr.

In table 1, we summarize the model parameters and initial conditions of our  $N$ -body simulations. Most of the parameters are the same as that used in H03. We chose the initial

velocity slightly larger than what is used in H03, to keep the mass loss rate smaller. This choice allowed us to follow the evolution of satellite for more than 10 orbits.

## 2.2. *N*-Body Simulation

In the *N*-body simulation, both the parent galaxy and the satellite were expressed as self-consistent *N*-body models. The number of particles  $N$  of the parent is  $10^6$  and that of the satellite is  $5 \times 10^4$ . The number of particles in the satellite should be large enough that the relaxation effect does not seriously affect the mass loss from the satellite. Since the initial half-mass relaxation time of the satellite is about 160 in our system of units, relaxation effect is small.

The number of particles in the parent galaxy should be determined so that the two-body relaxation effect on particles in the parent galaxies and those in satellite galaxies is small compared to the velocity dispersion of particles. Since the velocity dispersion of particles in the parent galaxy is much higher than the internal velocity dispersion of satellite particles, we only need to consider the heating of satellite particles due to encounters with particles in the parent galaxy. This heating rate is, for the first-order approximation, expressed as

$$T_h = t_{rc,p} \frac{\sigma_s^2}{\sigma_p^2}. \quad (3)$$

For our choice of initial model and number of particles,  $T_h \sim 10^3$  and it is sufficiently longer than the duration of the simulation.

We used a Barnes-Hut treecode (Barnes & Hut 1986; Makino 2004) on GRAPE-6A (Fukushige et al. 2005). We used opening angle  $\theta = 0.75$  with center-of-mass (dipole-accurate) approximation. The maximum group size for GRAPE calculation (Makino 1991) is 8192. For the time integration a leapfrog integrator with a fixed stepsize of  $\Delta t = 1/256$  is used.

To calculate the mass and orbit of the satellite, we need to identify the particles which belong to the satellite. We determine these particles by an iterative procedure (Funato et al. 1993). One particle belongs to the satellite if its binding energy to the satellite is negative. Potential energy is calculated using all other particles which belong to the satellite, and kinetic energy is calculated relative to the center-of-mass motion of the satellite.

## 2.3. Semianalytic Integration

We performed semianalytic calculations to follow the evolution of the satellite orbits. Our procedure is the same as that used in H03. The satellite is modeled as a single particle with variable mass and size, and the parent as a fixed gravitational potential. The potential of the parent is King 9 model with the same mass and scale as those used in the *N*-body simulations.

For the dynamical friction, we used the standard dynamical friction formula (Chandrasekhar 1943; Binney & Tremaine 1987), which is expressed as follows.

**Table 1.** Model Parameters of  $N$ -body Simulations

Parameters	Parent	Satellite
Galactic halo	King 9	King 7
Total mass	1.0	0.01
Binding energy	0.25	$0.25 \times 10^{-3}$
N	$10^6$	$5 \times 10^4$
Initial position		( 1.5, 0, 0)
Initial velocity		( 0, 0.45, 0)

$$\frac{d\mathbf{v}_s}{dt} = -16\pi^2 G^2 m (M_s + m) \log \Lambda \frac{\int_0^{v_s} f(\mathbf{r}, v_m) d\mathbf{v}_m}{|\mathbf{v}_s|^3} \mathbf{v}_s. \quad (4)$$

Here,  $v_s$  is the velocity of the satellite,  $G$  is the gravitational constant (equal to unity in our system of units),  $M_s$  and  $m$  are the masses of the satellite galaxy and field particles of the parent galaxy, and  $f(\mathbf{r}, v)$  is the distribution function of field particles at the position of the satellite. We assumed that the velocity distribution is isotropic, which is true at least for the initial model of the parent galaxy. The term  $\log \Lambda$  is the Coulomb logarithm and we adopted the form proposed by H03.

$$\log \Lambda = \log \left( \frac{R_s}{1.4\epsilon_s} \right), \quad (5)$$

where  $R_s$  is the distance between the center of the parent galaxy and the satellite galaxy and  $\epsilon_s$  is the size of the satellite.

In equations (4) and (5), we use the self-bound mass and virial radius of the satellite galaxy as  $M_s$  and  $\epsilon_s$ . For these quantities, we used the values obtained in  $N$ -body simulations.

### 3. Simulation Result

Figure 1 shows the snapshots of satellite galaxy projected onto the x-y plane. Initially, the satellite is located at distance 1.5 from the center of the parent galaxy. At  $t = 3$ , it is close to the first pericenter passage. Due to the strong tidal field of the parent galaxy, the satellite becomes elongated. At  $T = 9$ , particles stripped inward and outward form clear tidal arms, and the leading arm starts to form circular ring. As time proceeds, more and more mass is stripped out and at the same time the orbit of the satellite shrinks. At  $T = 24$ , stripped particles form complex collection of rings and spiral patterns.

Figure 2 shows the evolution of the bound mass of the satellite. At each pericenter passage, a significant amount of mass is lost. After the pericenter passage at around  $T = 45$ , the satellite is disrupted.

Figure 3 shows the orbital evolution of the satellite. Even though we adopted the prescription for Coulomb logarithm proposed by H03, the agreement between the  $N$ -body

simulation result and the result of semianalytic orbit integration is rather poor. After the first pericenter passage, the decrease of the apocenter distance is smaller by about a factor of two for the semianalytic integration. This factor-of-two difference continues to exist for entire simulation period.

This is a rather striking result. Jiang and Binney (2000) performed similar comparison between an  $N$ -body simulation and a semianalytic calculation, and their result was that the semianalytic calculation resulted in faster orbital evolution. They used constant  $\log \Lambda$  and this must be the cause of the difference. We used distance-dependent  $\log \Lambda$  of H03, and we found that the result is over-corrected. The semianalytic model resulted in the orbital evolution much slower than the result of the  $N$ -body simulation.

We have performed many simulations with different initial orbits and initial satellite model, but for all cases the result is similar. When mass loss from the satellite is significant, the semianalytic model of H03 failed to reproduce the orbit.

#### 4. Interaction between escaped particles and the satellite

Since the difference between the H03 model and our  $N$ -body simulation is that we used self-consistent model for the satellite, the cause of the discrepancy must be the interaction between the orbital motion of the satellite and its internal motion.

For example, a satellite is dynamically heated by “bulge shock” (Spitzer 1987) at each pericenter passage. The energy used to heat the internal motion of the satellite must have come from the orbital motion.

However, internal energy of the satellite is much smaller than the orbital energy and not enough to explain the orbital evolution. In the following, we consider two mechanisms which are potentially more efficient than simple heating of internal motion.

The first one is the interaction between the escaped particles and the satellite. In figure 1, particles escaped outward form rather impressive trailing spiral arms, while particles escaped inward form ring-like structure. This means the gravitational interaction between the escaped particles and the main body of the satellite is not symmetric. To the trailing spiral arm, the satellite exerts some tidal torque, since the angular velocity of the satellite is faster than that of the arm. On the other hand, the ring would not exert much torque to the satellite, since it is axisymmetric. This mechanism is essentially the same as the effect of non-conserving mass transfer from a binary of two stars. The gas escaped from the  $L_2$  point acquires the angular momentum through the interaction with the orbital motion of the binary, resulting in the loss of the orbital angular momentum of the binary. In this paper we call this effect the direct interaction between the escaped stars and the satellite.

The second mechanism is what we call “indirect interaction”. Many of the particles which are stripped out of the satellite remain close to the satellite. This is part of the reason why the direct interaction can be important. If escapers quickly go away from the satellite, the

energy and angular momentum loss due to the tidal torque would be small.

If some of the escapers remain close to the satellite, they might result in the enhancement of dynamical friction. One way to understand dynamical friction is to regard it as the gravitational pull by the wake of particles caused by the satellite galaxy. The strength of the wake depends on the mass which causes the wake. If some escaped particles remain close to the satellite, they help making the wake, resulting in the enhancement of the dynamical friction.

In the following two sections, we evaluate quantitatively these two effects in turn.

#### 4.1. Direct interaction with escapers

Here, we measure the effect of the direct interaction. The acceleration (or deceleration) of the satellite by the interaction with the escaped particle is defined simply as

$$\mathbf{a}_{\text{di}} = \frac{1}{M_s} \sum^i \sum^j \mathbf{f}_{ij}, \quad (6)$$

where the summation for  $i$  is taken for particles which escaped from the satellite, and summation over  $j$  is for particles which are bound to the satellite. The force  $\mathbf{f}_{ij}$  is simply the gravitational force from particle  $i$  to particle  $j$ .

We calculate change in the specific orbital energy by this direct interaction as

$$\Delta E_{\text{di}} = \int_0^T \mathbf{a}_{\text{di}} \cdot \mathbf{V} dt, \quad (7)$$

where  $\mathbf{V}$  is the velocity of the satellite.

Figure 4 shows the time change of  $\Delta E_{\text{di}}$ . For comparison, we also show the energy change due to dynamical friction  $\Delta E_{\text{df}}$  calculated using equation (4) and the specific total energy change  $\Delta E_{\text{total}}$  obtained directly from  $N$ -body simulation. Here,  $\Delta E_{\text{total}}$  is defined as

$$\Delta E_{\text{total}} = \int_0^T (\mathbf{a}_s - \mathbf{a}_p) \cdot \mathbf{V} dt, \quad (8)$$

where  $\mathbf{a}_s$  is the center-of-mass acceleration of the satellite,  $\mathbf{a}_p$  is the acceleration due to the potential of the parent, which is written as

$$\mathbf{a}_p = -\frac{GM(r)}{r^3} \mathbf{r}, \quad (9)$$

where  $r$  is the distance from the center of mass of the parent to that of the satellite,  $M(r)$  is the mass of the parent within  $r$ .  $M(r)$  is calculated from the density profile of the King model  $W_0 = 9$ , which is the same model as the parent halo in our  $N$ -body simulations.

We also show the sum of  $\Delta E_{\text{df}}$  and  $\Delta E_{\text{di}}$ . The pure dynamical friction accounts for about 70% of the total deceleration, and the direct interaction accounts for about half of the remaining energy change. Thus, we can conclude that the direct interaction is significant, but other effects are not negligible. In the next section we analyze the indirect contribution of escaped particles.

#### 4.2. Enhancement of the dynamical friction

Particles which have been stripped out of the satellite but still are close to it can increase the dynamical friction to the satellite, simply by being close.

To illustrate this effect, let us consider the simplest case, in which two softened point-mass objects move in a uniform distribution of field particles. Figure 5 shows the configuration we consider. Two massive objects,  $S_1$  and  $S_2$ , with equal masses  $M$ , move along  $z$  axis with velocity  $V_0$ . To simplify calculations, let us consider the case that field particles are at rest and distributed uniformly and isotropically. We calculate the enhancement of dynamical friction acting on  $S_1$  as a function of the distance between  $S_1$  and  $S_2$  in the following way.

The acceleration of  $S_1$  due to dynamical friction is given by

$$\frac{d\mathbf{v}_1}{dt} = n\mathbf{V}_0 \int_0^{b_{\max}} \int_0^{2\pi} \Delta\mathbf{V}_{1\parallel} b_1 d\theta_1 db_1, \quad (10)$$

where  $n$  is the number density of the field particles,  $\mathbf{V}_0$  is the initial velocity vector of  $S_1$ ,  $\Delta\mathbf{V}_1$  is the change in velocity of  $S_1$  caused by one encounter with a background particle,  $\Delta\mathbf{V}_{1\parallel}$  is the component of  $\Delta\mathbf{V}_1$  parallel to  $\mathbf{V}_0$ ,  $b_1$  is an impact parameter, and  $b_{\max}$  is the largest impact parameter. (Hereafter  $\parallel$  and  $\perp$  mean the components parallel and perpendicular to  $\mathbf{V}_0$ , respectively.) Note that we use  $b$  and  $\theta$  as integration variables, which means we chose a circle with the center at the center of coordinate in figure 6 as the region over which we integrate the encounters. By doing so, we made the integration region symmetric for two bodies.

For one encounter, from the momentum conservation, we have

$$M\Delta\mathbf{V}_{1\parallel} + M\Delta\mathbf{V}_{2\parallel} + m\Delta\mathbf{V}_{m\parallel} = 0. \quad (11)$$

Here,  $m$  is the mass of a background particle and  $\Delta\mathbf{V}_m$  is its velocity change. Figure 6 shows the view of the two massive particles and one background particle, on the plane perpendicular to the direction of the motion of massive particles. Since the configuration is symmetric for two massive particles, the dynamical friction on two particles, after integration in equation (10) is performed, must be equal. Thus, using equation (11), we can replace  $\Delta\mathbf{V}_1$  in the right-hand side of equation (10) as

$$\Delta\mathbf{V}_{1\parallel} = -\frac{m}{2M}\Delta\mathbf{V}_{m\parallel}. \quad (12)$$

In the following, we derive the formula for  $\Delta\mathbf{V}_{m\parallel}$  using impulse approximation. It is expressed as

$$\left| \frac{\Delta\mathbf{V}_{m\parallel}}{\mathbf{V}_0} \right| = 1 - \cos\psi, \quad (13)$$

where  $\psi$  is the deflection angle of the background particle and is expressed as

$$\psi = \left| \frac{\Delta\mathbf{V}_{m\perp}}{\mathbf{V}_0} \right|. \quad (14)$$

We can calculate  $\Delta\mathbf{V}_{m\perp}$  using the impulse approximation and by linearly adding the contribution of two massive bodies,  $\Delta\mathbf{V}_{m1}$  and  $\Delta\mathbf{V}_{m2}$  as

$$\Delta \mathbf{V}_{m\perp} = \Delta \mathbf{V}_{m1\perp} + \Delta \mathbf{V}_{m2\perp}, \quad (15)$$

$$\Delta \mathbf{V}_{m1\perp} = \frac{2G(M+m)}{V_0} \frac{b_1}{b_1^2 + \epsilon^2} \hat{\mathbf{b}}_1, \quad (16)$$

$$\Delta \mathbf{V}_{m2\perp} = \frac{2G(M+m)}{V_0} \frac{b_2}{b_2^2 + \epsilon^2} \hat{\mathbf{b}}_2, \quad (17)$$

where  $\epsilon$  is the softening length and  $\hat{\mathbf{b}}_1$  and  $\hat{\mathbf{b}}_2$  are the unit vectors in the directions from  $m$  to  $S_1$  and  $S_2$  on  $xy$ -plane.

Using these formulae, we numerically calculated the dynamical friction on  $S_1$  as a function of the distance between two massive particles  $d$ . Figure 7 shows the enhancement  $\beta$ , defined as the increase of the dynamical friction relative to the dynamical friction of single particle moving alone, as the function of the separation  $d$ . Here,  $d_0$  is defined as follows:

$$d_0 \equiv \frac{MG}{V_0^2}. \quad (18)$$

We adopt  $b_{\max}/d_0 = 100$  and  $\epsilon/d_0 = 5.0$ .

From figure 7, we can see that the increase of the dynamical friction is significant, even when two particles are far away (more than 10 times the softening length).

From this result, we estimated the enhancement of the dynamical friction on the satellite due to the escaped particles. The enhancement factor  $\alpha$  is calculated as

$$\alpha = \frac{1}{M_s} \int_0^{R_s} dr \frac{dm_e}{dr} \beta(r), \quad (19)$$

where  $m_e$  is the total mass of escaped particles within radius  $r$  from the center of mass of the satellite and  $\beta(r)$  is the value of  $\beta$  at distance  $r$ . Note that we made many approximations. First, we approximate the effect of particles at distance  $r$  in all directions by that of one particle in the plane perpendicular to the direction of motion. Second, we assume the linear relationship between the mass of the other particle and the enhancement of the dynamical friction. Third, we assume that the effect of multiple particles in different positions can be linearly added.

We performed the semianalytic orbital integration using the dynamical friction enhanced by this parameter  $\alpha$ . We also took into account the direct effect of escapers which we discussed in the previous section. Figure 8 shows the result. The agreement between the  $N$ -body simulation and the semianalytic integration is excellent. Figures 9 and 10 show the same comparisons for simulations from different initial orbits for the satellite. In both cases, the agreement between our improved treatment and the simulation result is quite good.

## 5. Discussion

We studied the orbital decay of a satellite galaxy, using fully self-consistent  $N$ -body simulation in which both the satellite and its parent galaxy are expressed by  $N$ -body models. Our main finding is that the pure dynamical friction, estimated using Chandrasekhar's formula with the correct treatment of Coulomb logarithm, underestimates the drag force by around

30%. This rather large discrepancy is due to the effect of particles which are stripped out of the satellite by the tidal field of the parent galaxy. They induce the additional drag force through two mechanisms. The first one is the direct force, which escaped particles exert on the body of the satellite. The particles ejected outward are accelerated by the tidal torque of the satellite, and the satellite loses the energy and angular momentum through the back reaction. The second mechanism is the indirect enhancement of the dynamical friction by particles which are not bound but still in the orbits close to the orbit of the satellite. We found these two mechanisms have comparable contributions and the combined effect quantitatively agrees with the discrepancy between the result of the  $N$ -body simulation and the model calculation using pure dynamical friction.

Our result implies that a naive application of the Chandrasekhar's dynamical friction formula can result in a significant overestimate of the timescale of the orbital evolution of an object, if the mass loss from that object is significant.

In the case of a satellite galaxy, the mass loss due to the tidal field of the parent galaxy is almost always significant. Recent  $N$ -body simulation of the formation and evolution of CDM halos (Kravtsov et al. 2004; Kase H. et al. 2005 in preparation) showed that most of subhalos lose 90% or more of their initial mass after they become bound to the main halo. Thus, the mass loss they experience is typically much bigger than the mass loss occurred to our model satellite. So we can conclude that the effect of mass loss to the orbital evolution of real substructures or satellite galaxies is even bigger than what we found.

For star clusters, whether or not the effect of escaped particles are important is not clear. Both the timescale of the orbital evolution and that of mass loss are significantly longer than the orbital timescale within the cluster. Thus, we need more careful analysis to study these effects. In the case of very young clusters born close to the galactic center (Figer et al. 1999), we can expect the effect of the escapers to be significant, since the ratio between the cluster mass and the relevant mass of the parent galaxy (mass inside the location of the cluster) is not too different from that ratio between the satellite and the parent galaxy. For most of the numerical studies of star clusters, the pure dynamical friction formula has been used (e.g., Portegies Zwart and McMillan 2002; Baumgardt and Makino 2003; Gürkan and Rasio 2005) These works might have significantly overestimated the timescale of orbital evolution. We will study these cases in the forthcoming paper.

The authors thanks Hiroyuki Kase, Keigo Nitadori and Masaki Iwasawa for helpful discussions and useful comments on the manuscript. This research is partially supported by the Special Coordination Fund for Promoting Science and Technology (GRAPE-DR project), Ministry of Education, Culture, Sports, Science and Technology, Japan.

## References

[Barnes and Hut (1986)] Barnes, J., & Hut, P. 1986, *Nature*, 324, 446

[Baumgardt and Makino (2003)] Baumgardt, H., & Makino, J. 2003, *MNRAS*, 340, 227

[Binney and Tremaine(1987)] Binney, J., & Tremaine S. 1987, *Galactic Dynamics* (Princeton: Princeton Univ. Press), 424

[Bullock, Johnston (2005)] Bullock, J. M., & Johnston, K.V. 2005, *astro-ph/0506467*

[Chandrasekhar(1943)] Chandrasekhar, S. 1943, *ApJ*, 97, 255

[Figer et al. (1999)] Figer, D. F., Kim, S. S., Morris, M., Serabyn, E., Rich, R. M., & McLean, I. S. 1999, *ApJ*, 525, 750

[Fukushige et al. (2005)] Fukushige, T., Makino, J., & Kawai, A. 2005, *astro-ph/0504407*

[Funato et al. (1993)] Funato, Y., Makino, J., & Ebisuzaki, T. 1993, *PASJ*, 45, 289

[Gürkan, Rasio (2005)] Gürkan, M. A., & Rasio, F. A. 2005, *ApJ*, 628, 236

[Hashimoto, Funato and Makino (2003)] Hashimoto, Y., Funato, Y., & Makino, J. 2003, *ApJ*, 582, 196

[Heggie and Mathieu(1986)] Heggie, D.C., & Mathieu, R.D. 1986, in *The Use of Supercomputers in Stellar Dynamics*, ed. P. Hut, and S. McMillan (Lecture Notes in Physics 267; Berlin: Springer), 233

[Helmi et al. (1999)] Helmi, A., White, S. D. M., de Zeeuw, P. T. & Zhao, H. 1999, *Nature* 402, 53

[Ibata and Lewis (1998)] Ibata, R. A., & Lewis, G. F. 1998, *ApJ*, 500, 575

[Jiang and Binney (2000)] Jiang, I.-G., & Binney, J. 2000, *MNRAS*, 314, 468

[Johnston et al. (1995)] Johnston, K. V., Spergel, D. N. & Hernquist, L. 1995, *ApJ*, 451, 598

[Kase et al.(2005)] Kase, H., Funato, Y., & Makino, J. 2005, in preparation

[Kravtsov et al. (2004)] Kravtsov, A. V., Gnedin, O. Y., Klypin, A. A. 2004, *ApJ*, 609, 482

[Makino(1991)] Makino, J. 1991, *PASJ*, 43, 621

[Makino (2004)] Makino, J. 2004, *PASJ*, 56, 521

[Murai, Fujimoto (1980)] Murai, T., & Fujimoto, M. 1980, *PASJ*, 32, 581

[Portegies Zwart and McMillan (2002)] Portegies Zwart, S., & McMillan, S. L. W. 2002, *ApJ*, 576, 899

[Portegies Zwart et al. (2004)] Portegies Zwart, S. F., Baumgardt, H., Hut, P., Makino, J. & McMillan, S. L. W, 2004, *Nature*, 428, 724

[Spitzer (1987)] Spitzer, L. 1987, *Dynamical evolution of globular clusters* (Princeton: Princeton Univ. Press), 119

[van den Bosch et sl. (1999)] van den Bosh, F. C., Lewis, G. F., Lake, G., & Stadel, J. 1999 *ApJ*, 515, 50

[White (1976)] White, D. M. S 1976, *MNRAS*, 174, 467

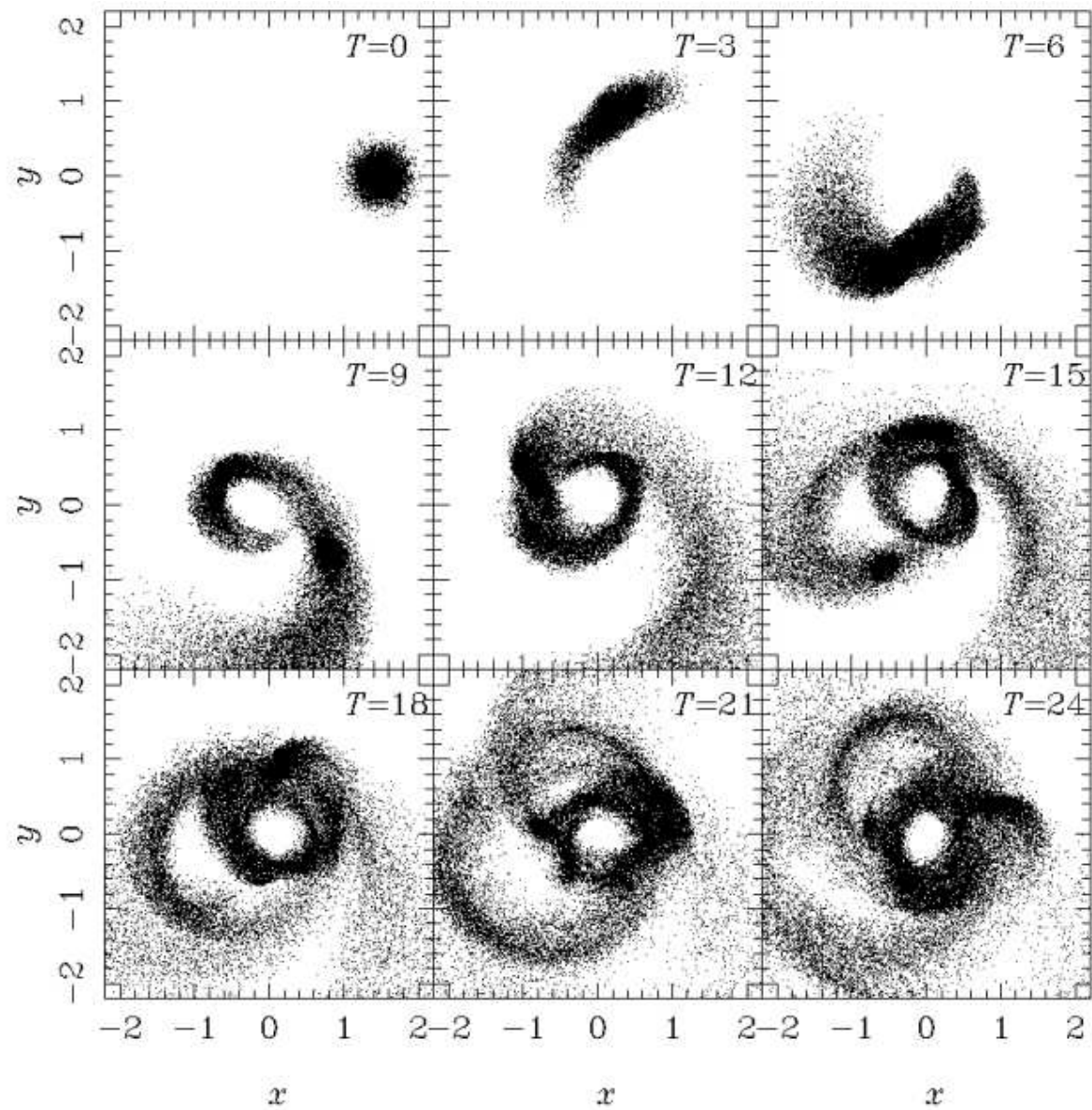


**Fig. 1.** Snapshots of the satellite particles projected onto the  $xy$ -plane.

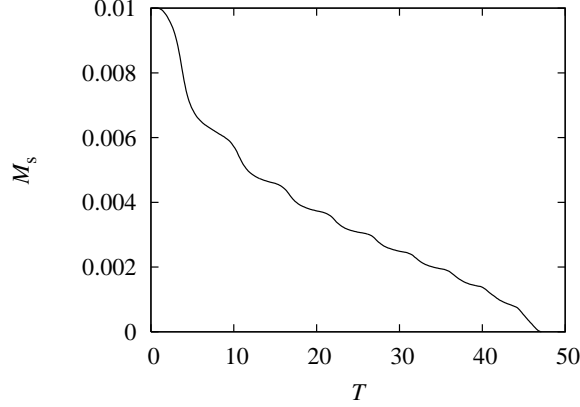


**Fig. 2.** Bound mass of the satellite  $M_s$  plotted as a function of time  $T$ .

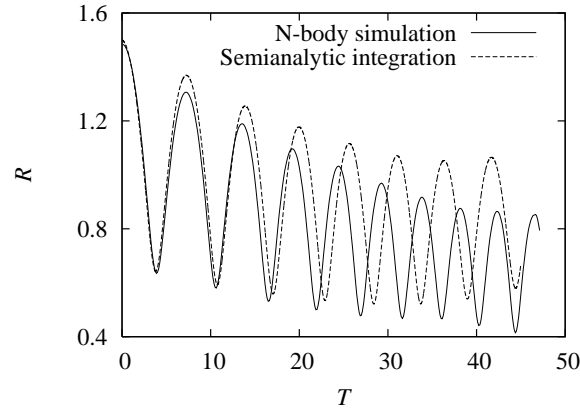


**Fig. 3.** The distance of the satellite from the center of the parent galaxy plotted as a function of time. Solid and dashed curves show the result of the  $N$ -body simulation and semianalytic integration, respectively.

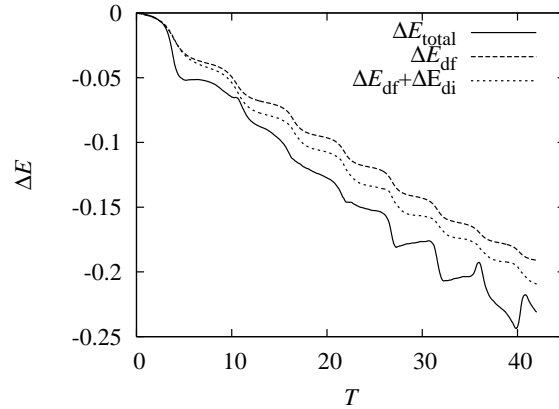


**Fig. 4.** The evolution of the orbital energy of the satellite plotted as the function of time. Solid curve shows the change of the orbital energy  $\Delta E_{\text{total}}$  obtained by the  $N$ -body simulation. Long-dashed curve shows the estimated energy change  $\Delta E_{\text{df}}$  due to the dynamical friction. Short-dashed curve shows the energy change due to the dynamical friction plus the direct effect of escaped particles  $\Delta E_{\text{df}} + \Delta E_{\text{di}}$ .

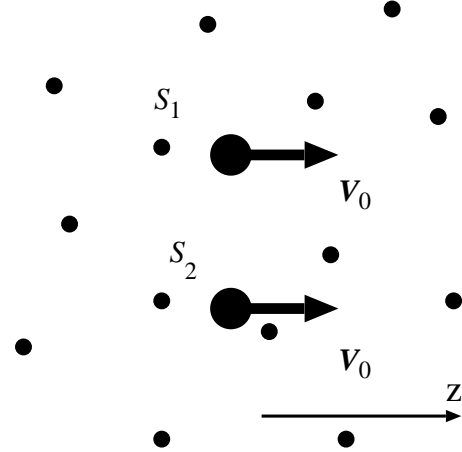


**Fig. 5.** Two massive objects moving in a uniform distribution of background field particles.

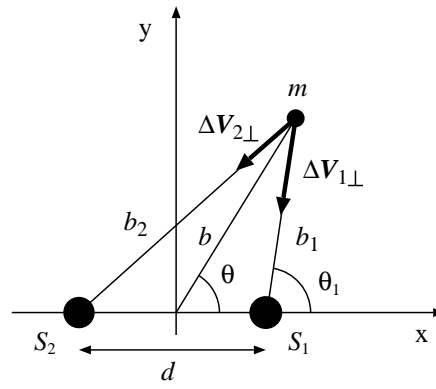


**Fig. 6.** View of two massive objects and one background particle on the plane perpendicular to the direction of motion of massive particles.

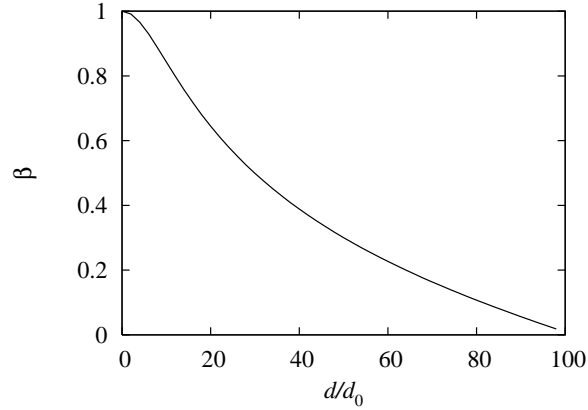


**Fig. 7.** The relative increase of the dynamical friction  $\beta$  as a function of the normalized distance between two objects.

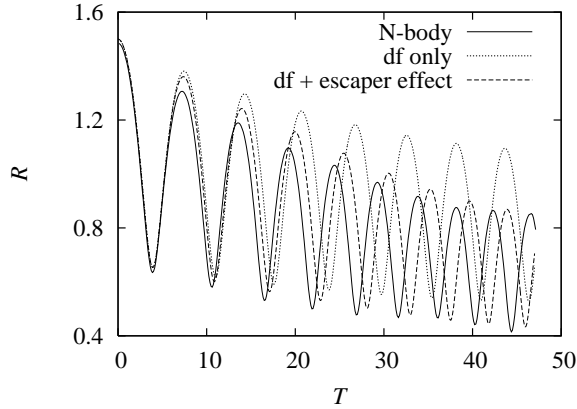


**Fig. 8.** Same as Fig. 3, but the result of semianalytic integration using only the pure dynamical friction is shown in the dotted curve and that with dynamical friction and both the direct and indirect effect of escapers is shown in the dashed curve.

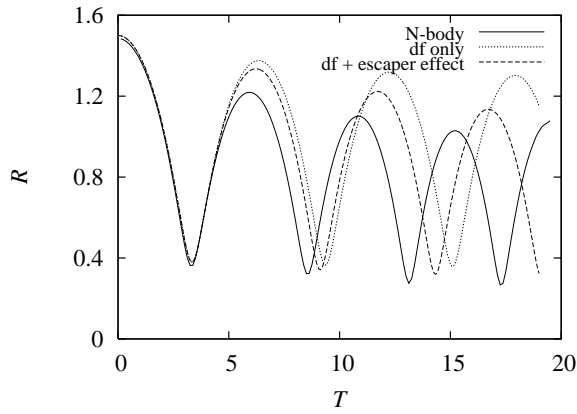


**Fig. 9.** Same as Fig. 8 but the initial velocity of the satellite is 0.326.

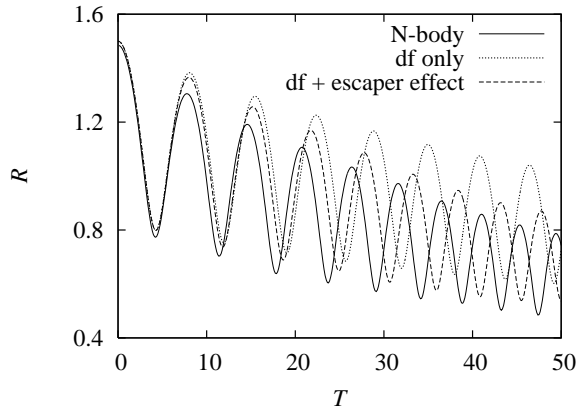


**Fig. 10.** Same as Fig. 8 but the initial velocity of the satellite is 0.5.